Heliyon 7 (2021) e08464

Contents lists available at ScienceDirect

Heliyon

journal homepage: www.cell.com/heliyon

Research article

Multiple conformations in solution of the maize C_4-phosphoenolpyruvate carboxylase isozyme

Fátima Barreda-Huerta [a], Ismael Bustos-Jaimes [b], Carlos Mújica-Jiménez [a], Rosario A. Muñoz-Clares [a,*]

[a] Departamento de Bioquímica, Facultad de Química, Universidad Nacional Autónoma de México, México DF, 04510, Mexico
[b] Departamento de Bioquímica, Facultad de Medicina, Universidad Nacional Autónoma de México, México DF, 04510, Mexico

HIGHLIGHTS

- PEP or malate binding produce distinct changes in *Zm*PEPC-C_4/ANS fluorescence.
- Different near-UV CD spectra of the free enzyme or of the enzyme complexes were observed.
- PEP or effectors binding produce distinctive *Zm*PEPC-C_4 trypsin-fragmentation patterns.
- Our results support several ligand-induced *Zm*PEPC-C_4 conformational states in solution.
- Predicted trypsin-cleavage sites are at flexible loops, which probably participate in *Zm*PEPC-C_4 function and regulation.

GRAPHICAL ABSTRACT

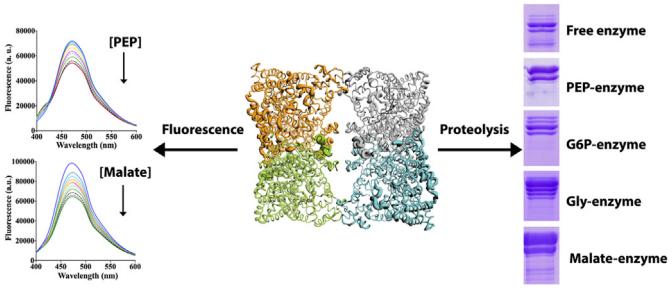

ARTICLE INFO

Keywords:
Zea mays L.
C_4 metabolism
Allosteric regulation
Ligand-induced conformational changes
ANS fluorescence
CD spectroscopy
Trypsin proteolysis

ABSTRACT

The photosynthetic phospho*enol*pyruvate carboxylase isozyme from C_4 plants (PEPC-C_4) has a complex allosteric regulation, involving positive cooperativity in binding the substrate phospho*enol*pyruvate as well as positive and negative allosteric effectors. Besides the proposed R- and T-states, previous kinetic results suggested functionally relevant different R-states of the maize enzyme (*Zm*PEPC-C_4) elicited by PEP or its two kinds of activators, glucose 6-phosphate or glycine. To detect these different R-state conformations, we used as conformational probes the fluorescence of 8-anilino-1-naphthalene sulfonate (ANS), near-UV circular dichroism (CD) spectroscopy, and limited proteolysis by trypsin. Phospho*enol*pyruvate and malate binding caused distinct concentration-dependent fluorescence changes of *Zm*PEPC-C_4/ANS, suggesting that they elicited conformational states different from that of the free enzyme, while glucose 6-phosphate or glycine binding did not produce fluorescence changes. Differences were also observed in the near UV CD spectra of the enzyme, free or complexed with its substrate or allosteric effectors. Additionally, differences in the trypsin-digestion fragmentation patterns, as well as in the susceptibility of the free and complexed enzyme to digestion and digestion-provoked loss of activity, provided evidence of several *Zm*PEPC-C_4 conformations in solution elicited by the substrate and the allosteric effectors. Using the already reported *Zm*PEPC-C_4 crystal structures and bioinformatics methods, we predicted that the most probable trypsin-cleavage sites are located in superficial flexible regions, which seems relevant for the protein

* Corresponding author.
E-mail address: clares@unam.mx (R.A. Muñoz-Clares).

https://doi.org/10.1016/j.heliyon.2021.e08464
Received 24 July 2021; Received in revised form 16 September 2021; Accepted 19 November 2021

dynamics underlying the function and allosteric regulation of this enzyme. Together, our findings agree with previous kinetic results, shed light on this enzyme's complex allosteric regulation, and place *Zm*PEPC-C_4 in the growing list of allosteric enzymes possessing an ensemble of closely related R-state conformations.

1. Introduction

In leaves of C_4 plants, two metabolic pathways are involved in the assimilation of the atmospheric CO_2: the C_4 and the Calvin cycles. In the C_4 cycle, the initial CO_2 assimilation reaction is the carboxylation of phospho*eno*lpyruvate (PEP) by the phospho*eno*lpyruvate carboxylase C_4-isozyme (PEPC-C_4), which yields oxaloacetate and inorganic phosphate in mesophyll cells of C_4 plants [1]. Oxaloacetate is then converted to malate or aspartate, depending on the plant, which are transported to the vascular sheath cells where they produce the CO_2 that is finally assimilated into sugars by the Calvin cycle in the chloroplast of these cells.

The importance of the PEPC-C_4 isozyme in the photosynthetic CO_2 assimilation metabolism of C_4 plants is underscored by its complex allosteric regulation —particularly in the case of PEPC-C_4 from gramineous C_4 plants such as the maize isozyme (*Zm*PEPC-C_4)—, which involves positive cooperativity in the binding of PEP and the positive and negative allosteric effectors [for reviews, see Refs. [2, 3, 4]. At physiological pH, *Zm*PEPC-C_4 is allosterically activated by phospho-sugars, as glucose 6-phosphate (G6P) [5, 6, 7, 8], and the neutral amino acids glycine (Gly) and serine (Ser) [6, 7, 8, 9, 10, 11], whereas is subjected to feedback inhibition by the dicarboxylic acid malate [12, 13]. The two kinds of *Zm*PEPC-C_4 allosteric activators are by no means redundant; they act as separate metabolic signals, both indicating the necessity of a more active C_4 cycle under different physiological conditions. Activation of *Zm*PEPC-C_4 by phospho-sugars would increase C_4 cycle flux to keep pace with an active Calvin cycle—which leads to the build-up of these phospho-sugars—so that the fluxes of both cycles are coordinated and the C_4 cycle does not limit the rate of CO_2 assimilation by the Calvin cycle. *Zm*PEPC-C_4 activation by the neutral amino acids glycine and serine—produced during photorespiration—also would increase the CO_2 supply to the bundle sheath cells, which in turn would diminish or abolish photorespiration, leading to an increased net CO_2 assimilation [14].

The allosteric regulation of *Zm*PEPC-C_4 has been proposed [15, 16] to conform to the symmetry two-state model of Monod, Changeux, and Wyman (MWC model) [17], which postulated that the substrate and allosteric activators shift the preexisting equilibrium between an inactive, or less active, T-state and an active, or more active, R-state, favoring the latter. However, previous kinetic studies [9, 18] suggested that the binding of PEP, G6P, or Gly elicits different R-state conformations of *Zm*PEPC-C_4, which are in equilibrium with the free enzyme, as schematized in Figure 1. The two kinds of activators were found to have a *V* effect and to be synergic rather than additive, which suggests that (i) the conformation of the enzyme saturated by its substrate PEP is different from that of the enzyme saturated by G6P or Gly, and (ii) this conformation is also different from that existing when the two activators are simultaneously bound to their respective allosteric sites. Moreover, while saturation of *Zm*PEPC-C_4 by G6P is unable to revert the inhibition caused by a physiological concentration of malate, saturation by Gly or Ser produces an enzyme almost as active as that in the absence of the inhibitor [9], again supporting the notion that the two kinds of activators, i.e., phospho-sugars and neutral amino acids, elicit different conformational states.

The so far reported crystal structures of *Zm*PEPC-C_4 in an active R-state are of a free enzyme (PDB code 1JQO) [19], of the enzyme-Gly complex (PDB code 5VYJ) [20], and of the enzyme-phosphoglycolate-G6P-Gly complex (PDB code 6MGI) [21]. These R-state structures show the correct conformation of the active site and G6P- and Gly-allosteric sites and a disorganized malate-allosteric site, contrary to the reported T-state *Zm*PEPC-C_4 structures, which show disorganized active and activator-allosteric sites and a properly formed malate-allosteric site with bound malate (PDB code 6U2T) or citrate (PDB code 6V3O) [Carrizosa E. I., González-Segura L., and Muñoz-Clares R. A., manuscript in preparation]. As expected, the differences between the R-state and T-state crystal structures are important and multiple, but the differences between the three R-state crystal structures (1JQO, 5VYJ, and 6MGI) are subtle. Thus,

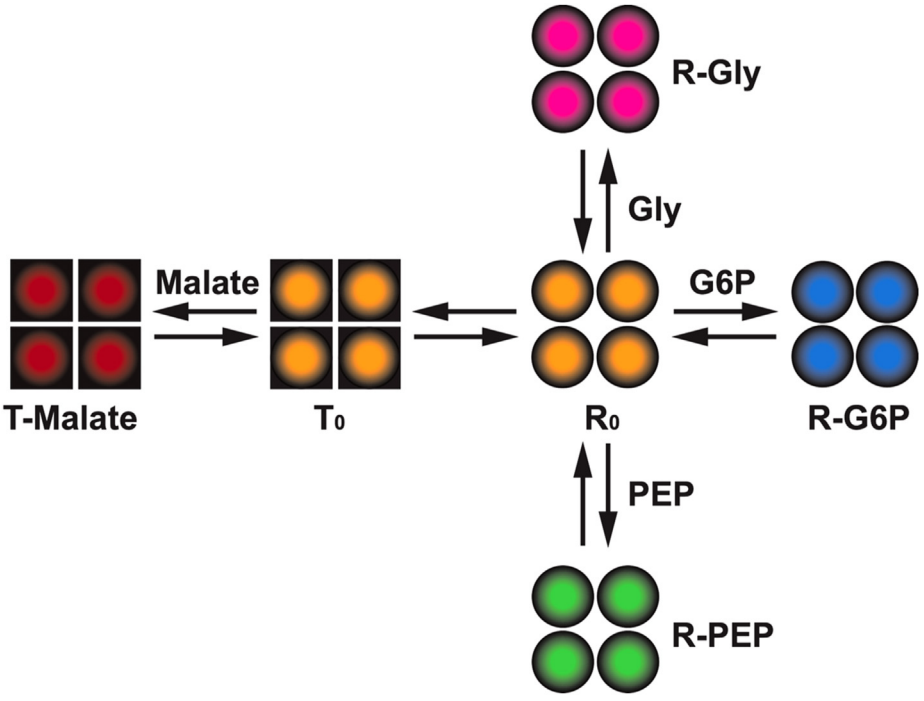

Figure 1. Schematic representation of the proposed different conformational states of *Zm*PEPC-C_4 and the equilibria between them. The free enzyme is assumed to predominantly be in the inactive T-state, which changes to a conformationally different malate-bound T-state in the presence of malate, or to different active R-sates in the presence of substrate or allosteric activators. Thus, we propose that the R-state adopts at least three different conformations depending on the binding of PEP, G6P, or Gly. It is likely that different conformations also exist when two or the three of the latter ligands are bound to their respective sites.

although the 1JQO structure has no substrate or allosteric activator bound, it has a similar overall conformation to the 6MGI structure, which has the PEP analog phosphoglycolate bound into the active site and G6P and Gly bound into their respective allosteric sites. The 5VYJ structure, which only has Gly bound in its allosteric site, also has a similar overall conformation, although it shows some differences with the other two R-state structures. Specifically, it differs in the degree of disorder of the loop forming the active site lid and in the conformation of the loop forming the G6P-allosteric site lid. Therefore, it appears that the functionally significant differences in the conformation or dynamics of the enzyme elicited by the substrate or the two kinds of activators, as indicated by the kinetic results, are lost in the crystal structures. The crystallization conditions might favor a single R-state conformation among the several energetically very similar—and therefore easily interconvertible—that probably exist in solution. Because of this, the possible different conformational R-states should be investigated through experiments carried out with the enzyme in solution. The size of this protein—a homotetramer of around 440 kDa—and the probable asymmetry of its subunits derived from high flexibility, as observed in the crystal structures, preclude the use of NMR spectroscopy. NMR using methyl labeling has been used for large proteins, but *Zm*PEPC-C_4 PEPC enzymes have several highly flexible regions in both the R- and T-states according to all reported crystal structures and, consequently, it is expected that they are not fully symmetrical. Indeed, the asymmetric unit in the reported crystal structures was two, four, or even eight. Each small difference between subunits will give different signals in the NMR experiments, and this will greatly complicate the analysis. For these reasons, to detect the conformational changes of *Zm*PEPC-C_4 induced by ligands, in this work we used three other experimental approaches: 1) Extrinsic fluorescence measurements using 8-anilino-1-naphthalene sulfonate (ANS) as a conformational probe; 2) near-UV circular dichroism (CD) spectroscopy, which gives information about changes in the tertiary structure of proteins affecting the surrounding environment of aromatic side chains; and 3) limited proteolysis, since a conformational change in the solution structure of the protein can lead to altered susceptibility to proteolysis. ANS fluorescence changes and limited proteolysis have been successfully used to detect different conformational changes induced by allosteric effectors of the *Escherichia coli* PEPC enzyme (*Ec*PEPC) [22, 23].

We here report that the substrate PEP changes the fluorescence of the *Zm*PEPC-C_4-ANS complex, while G6P and Gly did not, which suggests that the conformation of the PEP-bound R-state differs from those of the G6P-bound or Gly-bound R-states. We also observed differences in the near-UV CD spectra of the enzyme, free or complexed with its substrate or allosteric effectors. Furthermore, the fragmentation patterns of the enzyme in the absence and presence of PEP, G6P, or Gly were different from each other. Together, our results give strong support to the notion that *Zm*PEPC-C_4 has at least three different R-states, in accordance with previous kinetic results. Besides, based on the prediction of possible trypsin-cleavage sites, we propose the importance of certain flexible regions for the function and allosteric regulation of the enzyme.

2. Materials and methods

2.1. Expression, purification, and assay of recombinant ZmPEPC-C_4

The expression and purification of recombinant *Zm*PEPC-C_4 have been previously described [20]. Briefly, the cDNA for *Zm*PEPC-C*4* (*ppc-C4*, GenBank entry CAD60555, a kind gift from Dr. Katsura Izui) was subcloned into pET32a (+) vector (Novagen) between NcoI/HindIII restriction sites, as described [20]. The resulting plasmid was used for the expression of the full-length, N-terminal double-tagged thioredoxin and His6 *Zm*PEPC-C_4 protein in transformed BL21-CodonPlus (DE3)-RIL *E. coli* cells (Novagen). Protein purification was achieved by metal-affinity chromatography on a Protino nickel-tris(carboxymethyl) ethylene diamine column (Macherey-Nagel, Düren, Germany). After removal of the double tag by digestion at the thrombin cleavage site with enterokinase (New England Biolabs), the enzyme was further purified using a Mono QHR5 column (GE Healthcare) column. An ÄKTA™ PURE FPLC system (Cytiva) was used in the chromatographic steps. Protein concentration was determined spectrophotometrically by A280 using an extinction coefficient of 111,730 M^{-1} cm^{-1} predicted from the amino acid sequence using ExPASy ProtParam [24]. The purity of the recombinant *Zm*PEPC-C_4 was verified by SDS-PAGE after Laemmli [25]. The enzyme was stored at -80 °C in 50 mM HEPES-KOH buffer, pH 7.5, containing 10 mM 2-mercaptoethanol and 10% (v/v) glycerol until use. *Zm*PEPC-C_4 was assayed spectrophotometrically at 30 °C in a coupled enzymatic assay by monitoring NADH oxidation at 340 nm in 100 mM HEPES-KOH pH 7.3 buffer, 5 mM PEP, 10 mM CO_3H^-, 10 mM Mg^{2+}, 0.25 mM NADH and 4 units of malic dehydrogenase, in the absence or presence of allosteric effectors at the concentrations stated in each experiment.

2.2. Fluorescence measurements

ANS fluorescence was measured at 30 °C with a Shimadzu RF-5000 U spectrofluorimeter in 50 mM HEPES-KOH buffer, pH 7.3, 0.1 mM EDTA, 10 mM 2-mercaptoethanol, and 30 μM ANS. *Zm*PEPC-C_4 concentration was 150 μg/mL (1.37 μM as monomer) and PEP and allosteric effectors concentrations were varied as indicated in the text or the legends of the figures. ANS was excited at 370 nm and emission spectra were recorded between 400-600 nm at 2-min intervals after the addition of 5 μL ligand. The resulting spectra were corrected with those obtained upon the addition of 5 μL buffer. The corrected fluorescence intensities were used to calculate the dissociation constant of ligands by fitting the data to Eq. (1):

$$F = \{F_0 \times L_{0.5}^h / (L_{0.5}^h + [L]^h)\} + F_{min} \quad (1)$$

where F and F_o are the fluorescence intensities at the maximum wavelength of emission observed in the presence and absence of the ligand; respectively; [L] is the concentration of ligand; $L_{0.5}$ is the ligand concentration giving half of the maximum change in fluorescence, and equals the dissociation constant when the binding of the ligand is hyperbolic; F_{min} is the estimated residual fluorescence at saturation of the ligand; and h is the Hill number indicating the degree of cooperativity ($h = 1$ in hyperbolic binding; $h > 1$ in positive cooperativity binding). In these calculations, we used total instead of free ligand concentrations since the ligands were in great excess of the enzyme concentration, given their low affinity for the enzyme, and therefore their total concentrations are practically the same as their free concentrations.

2.3. CD spectroscopy

CD signals and dynode voltage were recorded with a Jasco J-715 spectropolarimeter (Jasco Inc., Easton, MD) equipped with a Peltier-type temperature control system (Model PTC-423S) and calibrated with d-10-(+)-camphorsulfonic acid. Near-UV (250–320 nm) spectra were recorded for solutions of 0.35 mg/ml protein concentration placed in quartz cuvettes of 0.5 cm path length. *Zm*PEPC-C_4 was in 10 mM HEPES buffer, pH 7.3, containing 0.5 mM 2-mercaptoethanol. Data were collected at 1 nm intervals, bandwidth of 1.0 nm, and a scan rate of 20 nm/min. Spectra were averaged over 3 scans, and the average spectrum of reference samples without protein was subtracted. The observed ellipticities were converted to molar ellipticities [Θ] on the basis of the molecular mass of the protein (109296.99 Da).

2.4. Limited proteolysis

Digestion of *Zm*PEPC-C_4 with trypsin was conducted at 25 °C in 100 mM HEPES-KOH, pH 7.3, containing 10 mM 2-mercaptoethanol, 1 mM EDTA, and 1 mM $CaCl_2$ at a protease to protein ratio of 1:100 (w/w). To follow the time-course of disappearance and formation of each proteolytic fragment, aliquots of the reaction mixture were withdrawn at

the indicated intervals, the reaction stopped with 1 mM phenylmethanesulfonyl fluoride (PMSF; Roche, USA) and immediately subjected to SDS-PAGE on 12 % polyacrylamide minislab gels after Laemmli [25]. Proteins were detected by staining with Coomassie blue R-250. The apparent molecular mass was estimated from SDS-PAGE gels comparing the relative migration with those of standard reference samples of known molecular mass (Bio-Rad, USA). In similar digestion experiments, after stopping the reaction with PMSF, aliquots were assayed for *Zm*PEPC-C_4 activity under standard assay conditions in the absence and presence of saturating concentrations of allosteric effectors.

2.5. Structural analysis

Docking simulations of ANS in the *Zm*PEPC-C_4 crystal structures 5VYJ (R-state with a glycine molecule bound into the neutral amino acids-allosteric site) and 6U2T (T-state with a malate molecule bound into the carboxylic acids-allosteric site) were attempted with DockingServer [26] (https://www.dockingserver.com/web) and Dockthor server [27] (https://dockthor.lncc.br/v2/). The glycine and malate molecules were removed from the corresponding pdb files before the docking simulations. Potential trypsin-cleavage sites were predicted with the Peptide-Cutter tool in the Expasy (Expert Protein Analysis System) web server [24] (http://expasy.org). The accessible surface area (ASA) was evaluated using the "Accessible Surface Area and Accessibility Calculation for Protein" tool (http://cib.cf.ocha.ac.jp/bitool/ASA/). Protruding atoms were identified using the Concave Finder program (http://cib.cf.ocha.ac.jp/bitool/CONCAVE/), which is based on the CX algorithm [28]. Cx values are the ratio between the external, exposed volume of atoms in a protein and the internal, buried volume (v_{ext}/v_{int}). Secondary structure elements of *Zm*PEPC-C_4 were assigned with the program Stride [29] (http://webclu.bio.wzw.tum.de/stride/). The proposed trypsin-cleavage sites were mapped on the crystal structure using PyMOL (http://www.pymol.org/).

3. Results and discussion

3.1. ANS fluorescence measurements

The binding of the substrate PEP or the allosteric effectors G6P, Gly, or malate did not induce any measurable change in the tryptophan fluorescence of *Zm*PEPC-C_4; thus intrinsic fluorescence could not be exploited to investigate ligand-induced conformational changes in solution. Therefore, to characterize the dynamic properties of *Zm*PEPC-C_4 upon ligand binding, we used the fluorescence probe ANS, which has a low fluorescence yield in aqueous solution but exhibits enhanced fluorescence when bound to hydrophobic sites on proteins [30].

In the absence of ligands, ANS binds to *Zm*PEPC-C_4 and produces an emission spectrum with a maximum at 476 nm (Figure 2 A, B). The allosteric activators G6P and Gly did not significantly affect the maximum *Zm*PEPC-C_4/ANS-fluorescence even at high concentrations (data not shown). Therefore, ANS is not adequate to detect the conformational changes elicited by these two kinds of allosteric activators. On the contrary, the substrate PEP and the allosteric inhibitor malate decreased the maximum *Zm*PEPC-C_4/ANS-fluorescence to a different extent (Figure 3 A, B). The fluorescence signal changes in response to the binding of PEP or malate are a function of ligand concentration (Figure 3 C, D). The corresponding fits of the fluorescence data to Eq. (1) yield the binding parameters given in the table included in Figure 3. The estimated $L_{0.5}$ value and the degree of binding cooperativity for PEP agree reasonably well with those previously found in experiments where the protection of the enzyme activity afforded by PEP against chemical modification by pyridoxal phosphate was measured [31]. Thus, the estimated $L_{0.5}$ and h values for PEP in the referred study were 5.33 ± 0.32 mM and 2.43 ± 0.33, respectively,

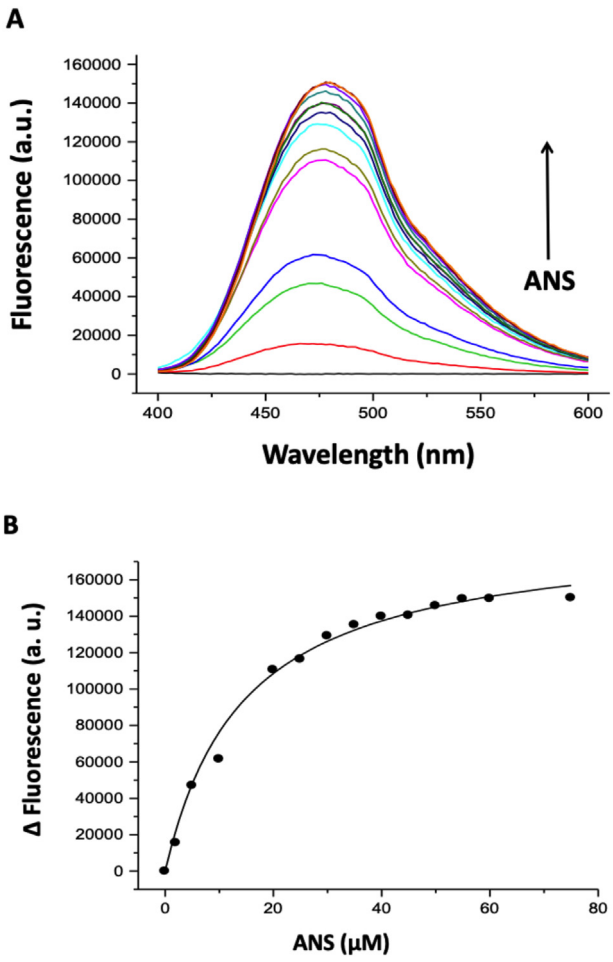

Figure 2. ANS-dependent fluorescence response in *Zm*PEPC-C_4. (A) Emission spectra of *Zm*PEPC-C_4/ANS solutions in the presence of increasing concentrations of ANS. The protein concentration was 1.37 μM as monomer. ANS was excited at 370 nm. Spectra were corrected with those of the buffer. (B) ANS-concentration dependence of the fluorescence signal at 476 nm. The dissociation constant (K_d) of the ANS-*Zm*PEPC-C_4 complex was calculated by fitting the data to $y = y_{max}$*[ANS]/(K_d + [ANS]), where y are the fluorescence data. The estimated K_d value was 14.5 ± 1.5 μM.

while the values estimated by ANS fluorescence in the present study are 5.42 ± 0.62 mM and 3.2 ± 0.9, respectively. Similarly, the estimated binding parameters for malate are close to the reported inhibition parameters found for malate in initial velocity experiments: I_{50} 0.43 ± 0.04 mM and h 1 [32] versus $L_{0.5}$ 0.36 ± 0.07 mM and h 0.9 ± 0.2 in the present study.

The differences in the response of the enzyme upon binding of the two ligands—highly cooperative in the case of PEP and non-cooperative in the case of malate—suggest that the PEP-induced conformational state is different from the malate-induced conformational state, although both appear to be either more compact or with less hydrophobic patches exposed. Thus, the ANS-fluorescence data suggest that binding of PEP or malate induces two different allosteric transitions to conformational states different from that of the free enzyme: the one induced by the substrate PEP, which cooperatively shifts the equilibrium between the T_0 state present in the absence of ligands towards the PEP-bound R state, and the one induced by malate, which non-cooperatively induces or stabilizes a different T state, the malate-bound T state, as depicted in Figure 1. This finding is consistent with previously reported *Zm*PEPC-C_4 kinetic data, which showed cooperativity in PEP binding and non-cooperativity in malate binding [9, 32]. Also, the finding that the allosteric transition induced by either G6P or Gly did not affect ANS binding

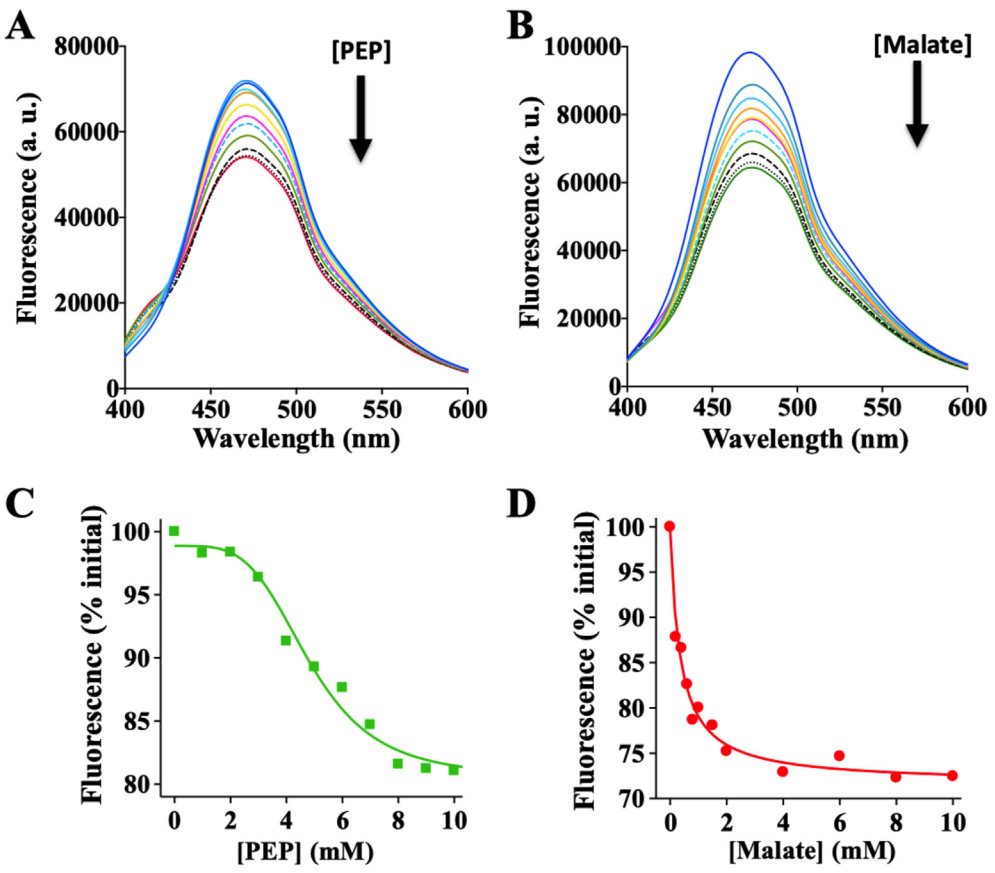

Figure 3. Extrinsic fluorescence studies. Emission spectra of *Zm*PEPC-C_4/ANS solutions in the presence of increasing concentrations of PEP (A), or malate (B). a.u., arbitrary units. (C and D) Ligand-concentration-dependent fluorescence changes. The lines are drawn from the best fit of the changes in fluorescence intensity at the maximum emission wavelength (476 nm) to Eq. (1), which gives the binding parameters shown in the table inserted in this figure. Fluorescence changes are expressed as a percentage of the fluorescence measured in the absence of ligand (F_0).

Ligand	F_{min} (%F_0)	$L_{0.5}$ (mM)	h
PEP	78.0 ± 3.1	5.42 ± 0.62	3.1 ± 0.9
Malate	70.7 ± 1.7	0.36 ± 0.07	0.9 ± 0.2

suggests differences between the PEP-bound R state and the G6P-bound or Gly-bound R states, but the possible differences between the two latter R states could not be studied using this technique.

We can not rule out the possibility that ANS binds to the active site or the malate-allosteric site and therefore that PEP and malate displace the fluorophore instead of inhibiting its binding through a conformational change. Nonetheless, we think that the probability of doing so is low given (i) the highly polar nature of the PEP- and malate-binding sites, although they could bind the sulfonic group of ANS; (ii) the good agreement of the values of the binding parameters with those determined by different experimental methods; and (iii) our failure to obtain by docking simulations the ANS molecule inside the active or malate-binding sites of the *Zm*PEPC-C_4 5VYJ (glycine-bound R state) or 6U2T (malate-bound T state) crystal structures (results not shown). Indeed, the best poses obtained showed that ANS binds at the protein surface, off of the active or allosteric sites; but again we are aware that dockings results are not conclusive proofs. But even if isosteric competitive binding caused the decreases in fluorescence of the *Zm*PEPC-C_4-ANS complex, our data represent a valuable contribution to the knowledge of the mode of binding of PEP and malate and the allosteric transitions elicited by them. But because the fluorescence results did not inform about possible differences between the conformational states triggered or stabilized by the two kinds of allosteric effectors of this enzyme, we tried different experimental approaches to detect the existence of the distinct conformational states suggested by the kinetic studies.

3.2. CD spectra

The CD spectra in the near-UV region of free or ligand-bound *Zm*PEPC-C_4 are shown in Figure 4A. To the best of our knowledge, this is the first report of CD spectroscopy performed in a PEPC enzyme. The considerable number of aromatic residues in *Zm*PEPC-C_4 (38 Phe, 27 Tyr, and 13 Trp per subunit) precludes a detailed analysis of the spectra. Nevertheless, the differences between these spectra (depicted in Figure 4B as the difference spectra obtained subtracting the CD spectrum of the free enzyme from the CD spectrum of each enzyme complex) suggest changes in the local environment of some of these residues and, therefore, different enzyme conformations. When compared with the free enzyme, the E-malate complex spectrum showed the most remarkable changes, but differences were also observed in the CD spectra of the E-PEP, E-G6P, and E-Gly complexes, not only relative to the spectrum of the free enzyme but also between them. These results confirm the change to a T-state bound conformation elicited by the inhibitor malate and support that several distinct R-state conformations are elicited by the binding of the substrate PEP or the two kinds of allosteric activators.

3.3. Fragmentation patterns obtained by limited proteolysis

To further assess the possible existence of different active R-state conformations characteristic of the different complexes of *Zm*PEPC-C_4 with its substrate or with any of its two kinds of allosteric activators, we

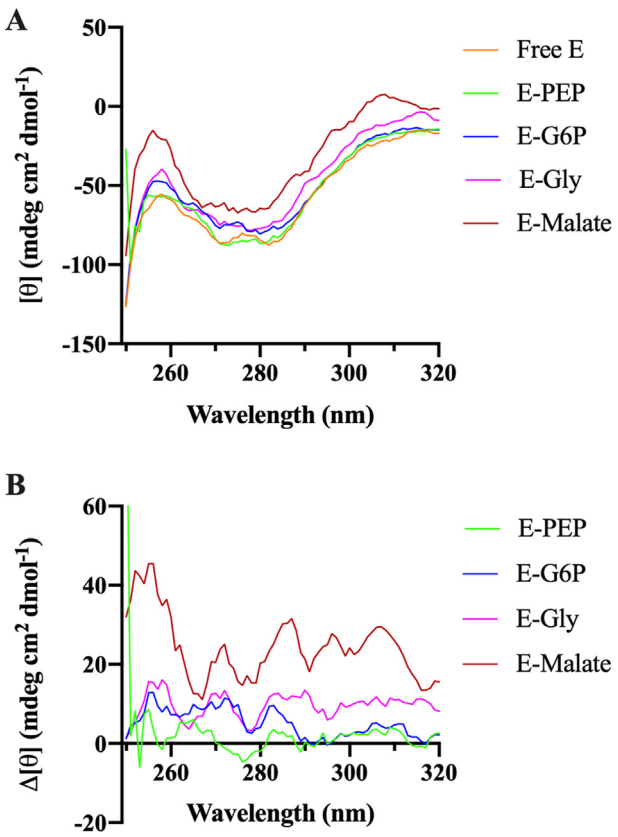

Figure 4. Circular dichroism studies. (A) Near-UV CD Spectra of *Zm*PEPC-C_4 in the absence or presence of the substrate PEP or allosteric effectors. (B) Near-UV CD difference spectra were obtained subtracting the CD spectrum of the free enzyme from the CD spectrum of each enzyme complex. Ligands concentrations were: 10 mM PEP, 15 mM G6P, 100 mM Gly, and 10 mM malate.

conducted limited proteolysis experiments by subjecting the protein loaded with PEP, G6P, or Gly to trypsin digestion and comparing the fragmentation patterns and the rates of fragment formation and degradation with those of the free, non-ligand-bound enzyme (Figure 5A). Similar experiments were performed with the enzyme-malate complex to test whether the inactive T-sate can also be detected using this experimental approach.

Trypsin quickly cleaved free *Zm*PEPC-C_4, while the ligand-bound enzyme forms were more resistant to digestion, particularly the complex enzyme-PEP. In the case of the free enzyme, after only 0.5 min incubation, a significant proportion of the intact protein was digested, producing a fragment of around 90 kDa, indicating a cleavage site very susceptible to trypsin proteolysis in the free enzyme. A second smaller fragment was also quickly formed, and after 60-min incubation, the protein was totally digested. The enzyme complexed with PEP was considerably more resistant to digestion, and the two major fragments formed, one of them in the first minutes of the incubation, accounted for almost all the initial amount of protein even after 120 min of incubation. In the enzyme-G6P complex, the intact protein was more quickly digested than in the enzyme-PEP complex, but not as quickly as in the free enzyme. After 15 min incubation, two major fragments were formed, but different from those formed in the complex enzyme-PEP, they were quite susceptible to further digestion. The digestion pattern of the enzyme-Gly complex is different from those of the enzyme-PEP and enzyme-G6P complexes, even though it would be expected the same active R-state in these three complexes if the MWC two-state allosteric model applied for *Zm*PEPC-C_4. After 15 min of incubation of the enzyme-Gly complex, three major fragments were formed. The amount of the fragment with the lower molecular mass increased with the digestion time and was very resistant to further proteolysis. It accounted for most of the undigested protein after 120-min incubation, suggesting that it has not accessible trypsin-cleavage sites or that its cleavage was considerably slow. Finally, the intact protein in the complex enzyme-malate was initially almost as resistant to trypsin as in the enzyme-PEP complex, but the major fragment formed is not as trypsin-resistant as the one formed when PEP is bound, so that a considerable number of smaller fragments were formed in the following minutes of incubation. This finding suggests that this major fragment is partially unstructured and exposes several new trypsin cleavage sites. After 120 min of digestion, the protein was almost completely digested.

Interestingly, the differences in the fragmentation patterns between free *Zm*PEPC-C_4 and its complexes with the substrate or allosteric effectors, as well as those between the four enzyme-complexes, were observed not only at the first minutes of incubation with trypsin but also at much longer times. Although we did not identify the different tryptic-cleavage sites in the studied enzyme complexes, the evolution of the fragmentation patterns during an extended time of incubation (up to 120 min) was also informative about the conformational states of *Zm*PEPC-C_4 elicited by its ligands. Our findings indicate that the different high-mass peptides formed at short times have different susceptibility to trypsin digestion and therefore seem not to have the same conformation despite apparently having similar masses.

In summary, the differences in the digestion patterns of the free *Zm*PEPC-C_4 enzyme and its different complexes indicate that some cleavage sites are more or less available for tryptic cleavage depending on the ligand-bound, thus revealing different conformational states in solution of this enzyme, as suggested by previous kinetic results. Thus, our results show that the trypsin digestion method is very sensitive to detecting different *Zm*PEPC-C_4 conformations in solution. It allowed the detection of not only those conformations expected to be very different, as the T-state elicited by the inhibitor malate and the R-state elicited by the substrate, but also those conformations that probably are slightly different, as the R-states elicited by the substrate or any of the two kinds of allosteric activators. Therefore, tryptic digestion might be a powerful and straightforward method for exploring the conformational space available in PEPC enzymes in particular and in enzymes subjected to allosteric regulation in general.

3.4. Effects of incubation with trypsin in the activity and sensitivity to allosteric effectors

To further substantiate the above-described results, we measured the residual activity and sensitivity to allosteric effectors of the free enzyme and the different enzyme complexes during their incubation with trypsin for 60 min. The loss of activity, expressed as the percentage of the activities of the free enzyme and different enzyme complexes measured at time zero of incubation with trypsin, are shown in Figure 5B. The changes in sensitivity to malate, expressed as the percentage of the enzyme inhibition by 10 mM malate measured at time zero of incubation, are shown in Figure 5C.

Consistent with the digestion patterns, important differences were found between the free and ligand-bound enzymes. The free enzyme rapidly lost activity—which agrees with the observed rapid digestion of the protein—while the enzyme in complex with PEP retained an important percentage of its initial activity, even after 60 min-incubation (Figure 5B). The latter finding suggests that at least one of the two fragments formed in the trypsin digestion of the enzyme-PEP complex, presumably the one with the higher molecular mass, has an intact active site. To find out whether these fragments conserved the quaternary tetrameric arrangement of the intact enzyme we subjected a sample of the enzyme-PEP complex to trypsin digestion for 60 min and then to size exclusion chromatography. But we could not obtain an elution profile because the protein was retained in the pre-column filter, suggesting that these fragments are highly hydrophobic and aggregated at concentrations above the low ones used in the activity assays. The enzyme-G6P and

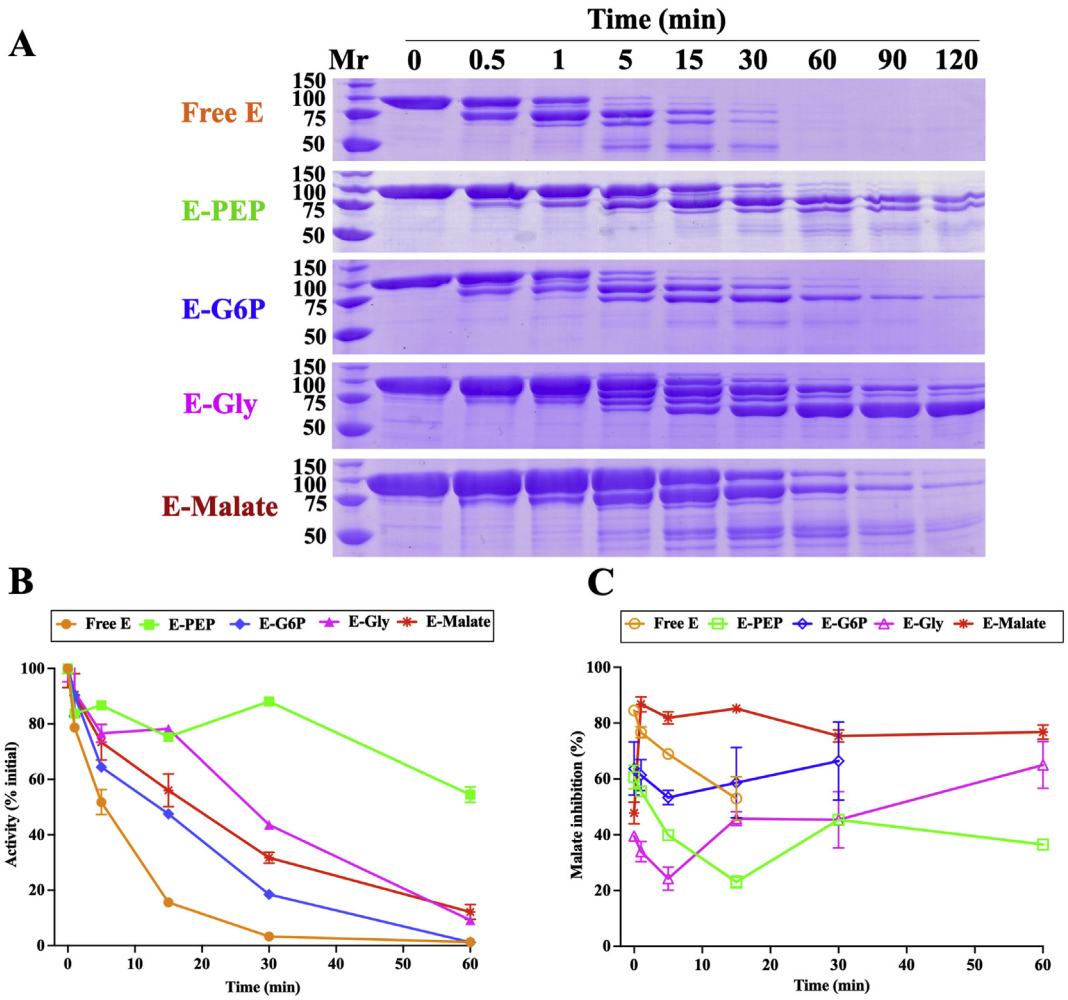

Figure 5. Limited proteolysis studies. *Zm*PEPC-C_4 was incubated with trypsin in the absence or presence of the substrate PEP or allosteric effectors and samples were withdrawn at the indicated times. The fragmentation patterns were visualized by SDS-PAGE (A), or the residual enzymatic activity was measured either in the absence of any effector (B) or in the presence of 10 mM malate (C). Ligands concentrations were: 10 mM PEP, 15 mM G6P, 100 mM Gly, and 10 mM malate. In panel B are given the average activities values measured using the standard assay at each time of incubation, expressed as the percentage of the average activity value measured at time zero, which as U/mg prot was: free-E = 0.633 ± 0.007; E-PEP = 0.975 ± 0.020; E-G6P = 1.251 ± 0.028; E-Gly = 1.036 ± 0.071; E-malate = 0.205 ± 0.014. In panel C are given the values of the percentage of inhibition by 10 mM malate measured at each time of incubation. The percentage of inhibition values at time zero were: free-E = 84.5 ± 0.2; E-PEP = 60.7 ± 4.2; E-G6P = 63.7 ± 9.5; E-Gly = 39.5 ± 1.4; E-malate: 47.8 ± 3.9. Some malate inhibition values at the longer times are not included in panel C because the activity in the absence of malate was so low that the determination of the degree of inhibition by malate was not reliable. The differences in the values at time zero between the free enzyme and the enzyme complexes are due to the presence of the ligands in the samples of the complexes. The full, uncropped versions of the SDS-PAGE gels shown in panel A are provided in the Supplementary Material (Fig. S1).

enzyme-Gly complexes were also more stable against trypsin-provoked activity losses than the free enzyme (Figure 5B). Gly afforded higher protection than G6P, probably because the amount of the intact protein remaining during the incubation is higher in the enzyme-Gly complex than in the enzyme-G6P complex. Finally, the stabilizing effects of malate were intermediate between those of G6P and Gly, a result also consistent with the higher stabilization afforded by this inhibitor against trypsin digestion of the intact protein.

In all enzyme complexes, the enzyme that remained active through the incubation appears to be equally sensitive to activation by G6P and Gly as at zero time (data not shown), but in the free enzyme and the PEP- and G6P- complexes a rapid partial loss of sensitivity to malate was observed within the first 5 min of incubation (Figure 5C). This reduced malate inhibition might result from the removal of an N-terminal fragment, as previously reported [33]. On the contrary, the sensitivity for malate of the enzyme-malate complex rapidly increased upon incubation with trypsin (Figure 5C) for a so far unknown reason. This interesting observation deserves further investigation since it could shed light on the structural bases of the mechanism of inhibition of PEPC enzymes by carboxylic acids.

3.5. Possible sites of trypsin cleavage

To further our understanding of the fragmentation patterns obtained, we next investigated the possible trypsin-cleavage sites in the *Zm*PEPC-C_4 protein using the bioinformatics methods described in the Materials and Methods section.

It is known that trypsin cleaves proteins on the C-terminal side of lysine or arginine [34], and a total of 119 potential cleavage sites were predicted in *Zm*PEPC-C_4 by the PeptideCutter tool. To narrow the selection of the probable cleavage-sites, and considering that the more accessible and protruding protein regions are the more likely to interact with trypsin, we carried out an analysis of the ASA and *cx* values of every protein residue using the available *Zm*PEPC-C_4 crystal structures (Figure 6 A, B; Fig. S2 A, B; Fig. S3 A, B; Table S1). As possible cleavage sites, we selected lysine and arginine residues that: (i) show the high ASA

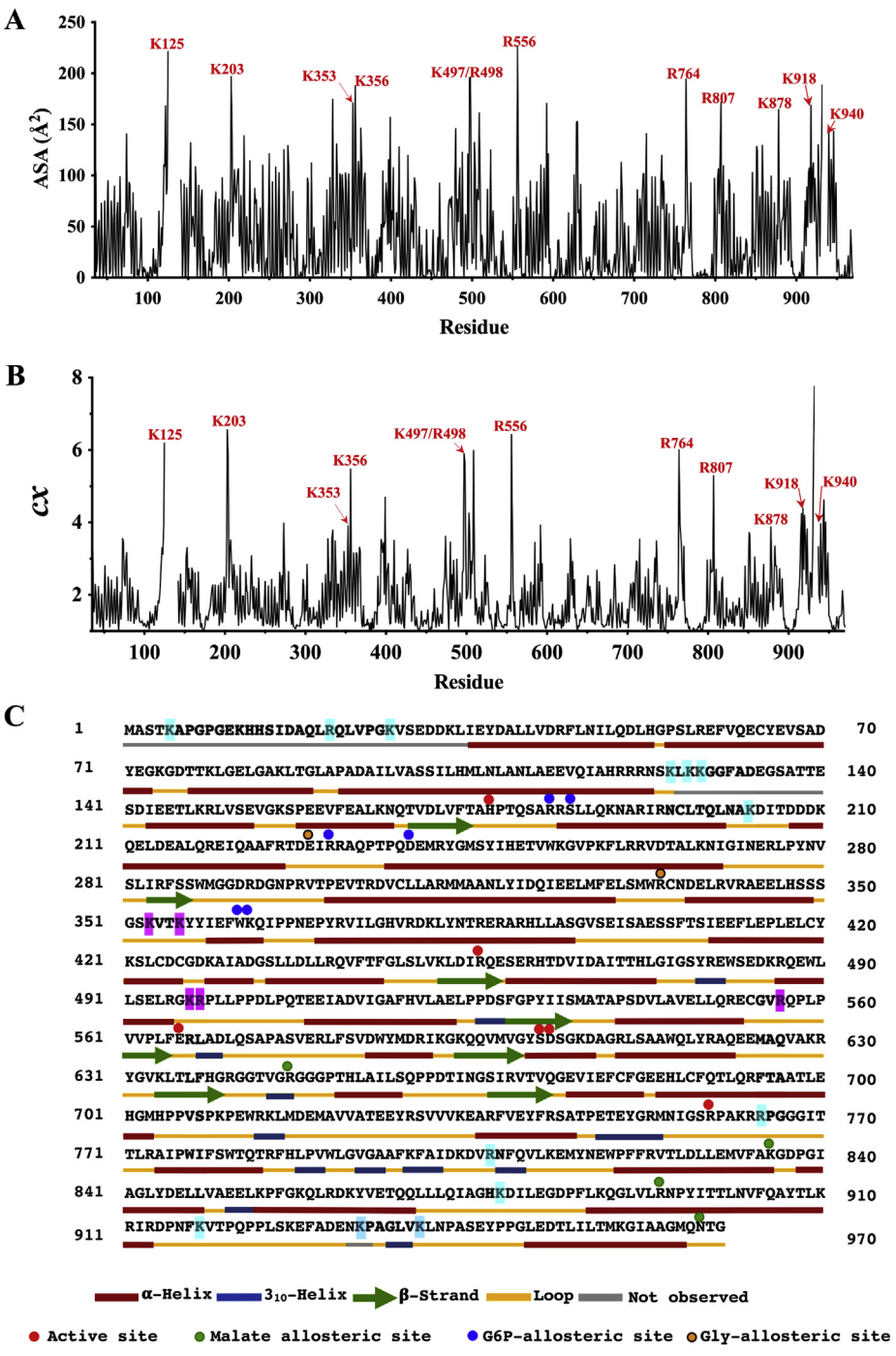

Figure 6. Prediction of trypsin-cleavage sites in *Zm*PEPC-C_4 5VYJ crystal structure. Of the three reported *Zm*PEPC-C_4 R-state structures, this is the one exhibiting more residues with associated electronic density. Shown are the results obtained using chain A. The residues of the trypsin-cleavage sites, predicted according to the criteria given in the text, are shown, and their ASA (A) and *cx* (B) values are indicated by red arrows. (C) Protein sequence and topology showing the position of the predicted cleavage sites. In cyan and magenta are marked the residues where the most and less likely cuts, respectively, could occur. Active site and allosteric sites residues are marked with colored circles to compare their positions in the protein sequence to those of the predicted trypsin-cleavage sites.

and *cx* values, (ii) are at flexible loops that could allow the binding at the active site of the protease [35, 36, 37], and (iii) do not have aspartate or glutamate at one or two positions before lysine or arginine, because it is known that they greatly slow the rate of hydrolysis [38]. We did not consider the "Keil rule", which proposes that cleavage does not occur if proline is after arginine or lysine [39], because this rule has been questioned given the abundance of cuts before proline in MS/MS data sets [40]. Applying these criteria, after a visual examination of the *Zm*PEPC-C_4 amino acid sequence and the topology of its crystal structures (Figs. 6C, S1C, and S2C), combined with the results of the ASA and *cx* analysis, we propose that the most likely cleavage sites are Lys125, Lys203, Lys353/Lys356, Lys497/Arg498, Arg556, Lys762/Arg763, Lys807, Lys878, Lys918, and Lys940. In addition, we propose that Lys5, Arg21, Lys27, and Lys127/Lys128 also are probable trypsin-cleavage sites since they are located in flexible regions—they did not show electronic density in any of the three reported R-state *Zm*PEPC-C_4 crystal structures—, and are not preceded by an acidic residue (Figs. 6C, S1C, and S2C, and Table S1). It seems reasonable to assume that, after cuts in the N-terminal segment, the peptide observed results from the cut at Lys27. Indeed, what we have called the intact enzyme in the experiments with the free enzyme and with the enzyme-PEP and enzyme-G6P complexes may be the one resulting from a cut at Lys27, which would be consistent with their rapid loss of sensitivity to malate, as mentioned. Nevertheless, in the enzyme-Gly complex, the complete protein could be the first band observed in the SDS-PAGE gels since malate sensitivity is retained. Cuts at Lys934 also are very likely. This is a very flexible residue, which is observed only in subunit A of the 6MGI structure where it is highly exposed.

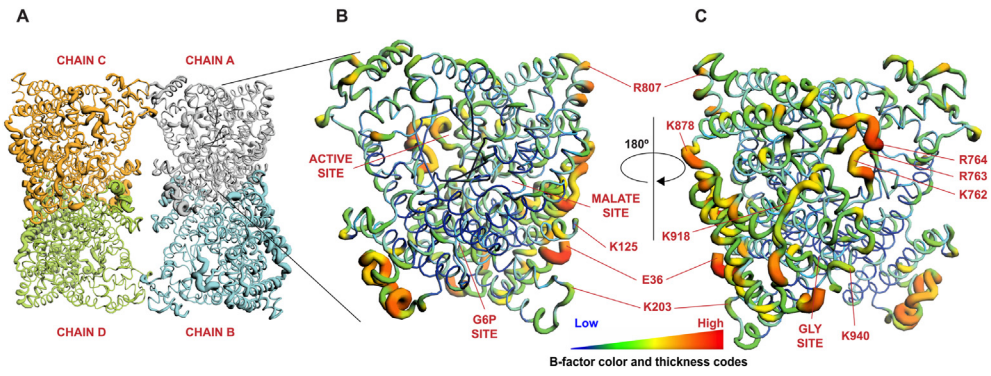

Figure 7. Mapping of the predicted trypsin-cleavage sites on the *Zm*PEPC-C_4 5VYJ crystal structure. Sausage B-factors representation of the tetramer showing static disorder in some loops. The structure is colored according to monomer in (A) and according to B-factors values in (B) and (C). Residues predicted as the most likely trypsin-cleavage sites are shown in panels (B) and (C) mapped in chain A. The position of the first residue observed in the N-terminal region (Glu36) and well as the positions of the active and allosteric sites are indicated in panel (B).

It is clear that in the protein sequence, the predicted trypsin-cleavage sites are not close to either active or allosteric sites residues, as shown in Figure 6C. Thus, to further explore the protein regions where the predicted cuts may occur, we mapped these cleavage sites on the three-dimensional structure of *Zm*PEPC-C_4 (Figure 7A) and found that neither are they close to the active site or allosteric sites (Figure 7 B, C). Therefore, it seems that the differences in their susceptibility to trypsin cleavage do not arise from protection by a particular ligand bound to the enzyme.

By visual inspection of the structure, it can be seen that cuts at Lys497/Arg498 and Arg556 cannot occur because they are located at the dimer-dimer interface of the tetramer (note that our predictions were based on these residues being highly exposed in the monomer used for the accessibility estimations) and therefore not accessible to the protease in the native enzyme. Similarly, cuts at Lys353/Lys356 are not probable since these residues are at the monomer interface in dimeric units. This deduction is consistent with the absence of digestion fragments of the corresponding size at the shorter incubation times. The other predicted cleavage sites are exposed in the tetramer and are located in very flexible regions or loops, as indicated by either their lack of electronic density or high Cα-B factor values compared with the average value (Figure 7 B, C). In particular, these sites are at 1) the N-terminal region—not observed in the three reported *Zm*PEPC-C_4 R-state crystal structures—, 2) at the Ser125- Ile144 loop—part of which is not observed in any of these R-state structures—, 3) at the Asn755-Arg773 loop that forms the active site lid—which is observed in the 5VYJ structure but is disordered at Lys762/Arg763/Arg764 in the 1JQO and 6MGI structures—, and 4) at the Pro915-Glu932 loop—which was completely observed only in subunit A of the 6MGI structure. In subunit B of the asymmetric unit of 6MGI and every subunit of 1JQO and 5VYJ, the short segment of Pro915-Glu932 loop not observed includes Lys934 (Figs. 6C, S1C, and S2C). A combination of cuts at the predicted trypsin-susceptible sites in these loops, plus the ones located in the flexible regions without electronic density in the crystal structures, could account for the observed digestion fragments in the different enzyme complexes, as shown in Table 1. Interestingly, it was reported that the incubation of the free *Ec*PEPC enzyme with trypsin produced a cut at Arg703 [41], which is the arginine residue equivalent to Arg763 of *Zm*PEPC-C_4 predicted by us as a highly possible cleavage site in the maize enzyme.

Table 1. Molecular masses of possible peptides obtained after tryptic digestion of *Zm*PEPC-C_4. Possible trypsin-cleavage sites were predicted according to the criteria stated in the text. Molecular masses were estimated using the ProtParam tool (https://web.expasy.org/protparam/). Only the peptides of high molecular mass (Mr) are included in this analysis. The intact recombinant enzyme used has 971 residues and a Mr value of 109,416 Da.

Peptide	Number of residues	Mr (Da)
K27-K940	912	103,267
K27-K934	907	102,857
K27-K918	891	101,075
K27-R878	851	96,385
K27-R807	780	88,116
K27-R764	737	83,306
K125-K940	814	92,447
K125-K934	808	91,882
K125-K918	792	90,100
K125-K878	753	85,565
K125-K807	682	77,297
K125-R764	639	72,487
K203-K940	736	83,850
K203-K918	714	81,502
K203-K878	675	76,968
K203-K807	604	68,699
K203-R764	561	63,889

Our findings of distinct trypsin-fragmentation patterns of the free enzyme and the different enzyme complexes suggest that the conformation of the above-mentioned flexible regions at the protein surface—which, as said before, are not directly involved in binding of the substrate PEP or of the allosteric effectors—are very sensitive to the binding of the different ligands. Also, they might play essential roles in the catalysis or allosteric regulation of the *Zm*PEPC-C_4 isozyme and, presumably, of plant PEPC enzymes in general. The N-terminal region before α1 and the loops mentioned above may also be necessary for bacterial PEPC enzymes. However, some of them are shorter than those present in the plant enzymes, as can be seen in the reported *Ec*PEPC crystal structures (PDB codes 1FIY, 1QB4, and 1JQN) [41, 42, 43]—an enzyme in which multiple conformational states have also been detected in solution [22, 23, 44, 45, 46]. The whole loop of the active site lid—to which Lys762/Arg763/arg764 (*Zm*PEPC-C_4 numbering) belong—is also present in the bacterial enzymes, and its amino acid sequence is highly conserved in both bacterial and plant PEPCs, supporting a critical role in the function of these enzymes.

Different conformations have been well documented in several allosteric proteins, particularly in hemoglobin, where closely related conformational states with different tertiary structures have been proposed to explain the binding properties of this protein [47, 48, 49, 50] and references therein]. Other allosteric enzymes may also present different R-states, as is the glucosamine-6-phosphate deaminase from *E. coli*, whose different R-states were demonstrated by fluorescence spectroscopy [51]. Regarding PEPC enzymes, the great conformational flexibility that gives rise to the multiplicity of ligand-induced, or ligand-stabilized, conformational states appears to be a general feature of PEPC enzymes and not only of the *Ec*PEPC previously reported.

4. Conclusions

The results from the combined experimental and bioinformatic methods used in this work support the existence of multiple

conformations of *Zm*PEPC-C_4 in solution and point out the importance of certain flexible regions at the protein surface for the PEPC enzymes dynamics underlying their function and allosteric regulation. Together, our results contribute to understanding the complex allosteric regulation of PEPC enzymes in general and of the plant *Zm*PEPC-C_4 isozyme in particular, which is an important biotechnological target in the efforts to increase crops yields.

Declarations

Author contribution statement

Fátima Barreda-Huerta: Performed the experiments; Analyzed and interpreted the data.

Ismael Bustos-Jaimes: Performed the experiments; Analyzed and interpreted the data; Contributed reagents, materials, analysis tools or data.

Carlos Mújica-Jiménez: Performed the experiments.

Rosario A. Muñoz-Clares: Conceived and designed the experiments; Analyzed and interpreted the data; Contributed reagents, materials, analysis tools or data; Wrote the paper.

Funding statement

Rosario A. Muñoz-Clares was supported by UNAM, grant PAPIIT IN216911. Fátima Barreda-Huerta was supported by a CONACYT scholarship.

Data availability statement

Data will be made available on request.

Declaration of interests statement

The authors declare no conflict of interest.

Additional information

Supplementary content related to this article has been published online at https://doi.org/10.1016/j.heliyon.2021.e08464.

Acknowledgements

We acknowledge the participation of the deceased Dr. G. Mendoza, Faculty of Medicine, UNAM, in preliminary mass spectrometry experiments.

References

[1] M.D. Hatch, C_4 photosynthesis: an unlikely process full of surprises, Plant Cell Physiol. 33 (1992) 333–342.
[2] C.S. Andreo, D.H. González, A.A. Iglesias, Higher plant phosphoenolpyruvate carboxylase: structure and regulation, FEBS Lett. 213 (1987) 1–8.
[3] R. Chollet, J. Vidal, M.H. OLeary, Phosphoenolpyruvate carboxylase: a ubiquitous, highly regulated enzyme in plants, Annu. Rev. Plant Physiol. Plant Mol. Biol. 47 (1996) 273–298.
[4] K. Izui, H. Matsumura, T. Furumoto, Y. Kai, Phosphoenolpyruvate carboxylase: a new era of structural biology, Annu. Rev. Plant Biol. 55 (2004) 69–84.
[5] K.F. Wong, D.D. Davies, Regulation of phosphoenolpyruvate carboxylase of *Zea mays* by metabolites, Biochem. J. 131 (1973) 451–458.
[6] H.D. Doncaster, R.C. Leegood, Regulation of phosphoenolpyruvate carboxylase activity in maize leaves, Plant Physiol. 84 (1987) 82–87.
[7] V. Bandarian, W.J. Poehner, S.D. Grover, Metabolite activation of crassulacean acid metabolism and C_4 phosphoenolpyruvate carboxylase, Plant Physiol. 100 (1992) 1411–1416.
[8] A. Tovar-Méndez, R. Rodríguez-Sotres, D.M. López-Valentín, R.A. Muñoz-Clares, Re-examination of the roles of PEP and Mg^{2+} in the reaction catalysed by the phosphorylated and non-phosphorylated forms of phosphoenolpyruvate carboxylase from leaves of *Zea mays*: effects of the activators glucose 6-phosphate and glycine, Biochem. J. 332 (1998) 633–642.
[9] A. Tovar-Méndez, C. Mújica-Jiménez, R.A. Muñoz-Clares, Physiological implications of the kinetics of maize leaf phosphoenolpyruvate carboxylase, Plant Physiol. 123 (2000) 149–160.
[10] T. Nishikido, H. Takanashi, Glycine activation of PEP carboxylase from monocotyledonous C_4 plants, Biochem. Biophys. Res. Commun. 53 (1973) 126–133.
[11] J. Gillinta, S.D. Grover, Kinetic interactions of glycine with substrates and effectors of phosphoenolpyruvate carboxylase from maize leaves, Photosynth. Res. 45 (1995) 121–126.
[12] S.C. Huber, G.E. Edwards, Inhibition of phosphoenolpyruvate carboxylase from C_4 plants by malate and aspartate, Can. J. Bot. 53 (1975) 1925–1933.
[13] D.H. González, A.A. Iglesias, C.S. Andreo, On the regulation of phosphoenolpyruvate carboxylase activity from maize leaves by L-malate. Effect of pH, J. Plant Physiol. 116 (1984) 425–434.
[14] R.C. Leegood, The intercellular compartmentation of metabolites in leaves of *Zea mays* L, Planta 164 (1985) 163–170.
[15] J. Frank, J. Vater, J.F. Holzwarth, Kinetics and equilibrium binding of phosphoenolpyruvate to phosphoenolpyruvate carboxylase from *Zea mays*, Phys. Chem. Chem. Phys. 1 (1999) 455–461.
[16] J. Frank, R.J. Clarke, J. Vater, J.F. Holzwarth, Influence of allosteric effectors on the kinetics and equilibrium binding of phosphoenolpyruvate (PEP) to phosphoenolpyruvate carboxylase (PEPC) from *Zea mays*, Biophys. Chem. 30 (2001) 53–64.
[17] J. Monod, J. Wyman, J. Changeux, On the nature of allosteric transitions. A plausible model, J. Mol. Biol. 12 (1965) 88–118.
[18] C. Mújica-Jiménez, A. Castellanos-Martínez, R.A. Muñoz-Clares, Studies of the allosteric properties of maize leaf phosphoenolpyruvate carboxylase with the phosphoenolpyruvate analog phosphomycin as activator, Biochim. Biophys. Acta 1386 (1998) 132–144.
[19] H. Matsumura, Y. Xie, S. Shirakata, T. Inoue, T. Yoshinaga, Y. Ueno, K. Izui, Y. Kai, Crystal structures of C_4 form maize and quaternary complex of *E. coli* phosphoenolpyruvate carboxylases, Structure 10 (2002) 1721–1730.
[20] L. González-Segura, C. Mújica-Jiménez, J.A. Juárez-Díaz, R. Güémez-Toro, L.P. Martínez-Castilla, R.A. Muñoz-Clares, Identification of the allosteric site for neutral amino acids in the maize C_4 isozyme of phosphoenolpyruvate carboxylase: the critical role of Ser-100, J. Biol. Chem. 293 (2018) 9445–9957.
[21] R.A. Muñoz-Clares, L. González-Segura, J. Andrés Juárez-Díaz, C. Mújica-Jiménez, Structural and biochemical evidence of the glucose 6-phosphate-allosteric site of maize C_4-phosphoenolpyruvate carboxylase: its importance in the overall enzyme kinetics, Biochem. J. 477 (2020) 2095–2114.
[22] T. Yoshinaga, Phosphoenolpyruvate carboxylase of *Escherichia coli*: studies on multiple conformational states elicited by allosteric effectors with fluorescence probe, 1-anilinonaphthalene-8-sulfonate, Biochim. Biophys. Acta 452 (1976) 566–579.
[23] I. Kameshita, K. Izui, H. Katsuki, Phosphoenolpyruvate carboxylase of *Escherichia coli*: effect of proteolytic modification on the catalytic and regulatory properties, J. Biochem. 86 (1979) 1–10.
[24] E. Gasteiger, A. Gattiker, C. Hoogland, I. Ivanyi, R.D. Appel, A. Bairoch ExPASy, The proteomics server for in-depth protein knowledge and analysis, Nucleic Acids Res. 31 (2003) 3784–3788.
[25] U.K. Laemli, Cleavage of structural proteins during the assembly of the head of bacteriophage T4, Nature 227 (1970) 680–685.
[26] Z. Bikadi, E. Hazai, Application of the PM6 semi-empirical method to modeling proteins enhances docking accuracy of AutoDock, J. Cheminf. 15 (2009) 1–16.
[27] C.S. De Magalhães, D.M. Almeida, H.J.C. Barbosa, L.E. Dardenne, A dynamic niching genetic algorithm strategy for docking of highly flexible ligands, Inf. Sci. 289 (2014) 206–224.
[28] A. Pintar, O. Carugo, S. Pongor, CX, an algorithm that identifies protruding atoms in proteins, Bioinformatics 18 (7) (2002) 980–984.
[29] D. Frishman, P. Argos, Knowledge-based protein secondary structure assignment, Proteins 23 (1995) 566–579.
[30] G.H. Dodd, G.K. Radda, 1-Anilinonaphthalene-8-sulphonate, a fluorescent conformational probe for glutamate dehydrogenase, Biochem. J. 114 (1969) 407–417.
[31] A. Tovar-Méndez, H. Yampara-Iquise, C. Mújica-Jiménez, R.A. Muñoz-Clares, Binding of ligands to the glucose-6-phosphate allosteric site in maize-leaf phopshoenolpyruvate carboxylase, in: P. Mathis (Ed.), Photosynthesis: from Light to Biosphere 5, Kluwer, Dordrecht, 1995, pp. 155–158.
[32] R. Güemez-Toro, C. Mújica-Jiménez, R.A. Muñoz-Clares, Allosteric regulation of the photosynthetic C4 isoenzyme of phosphoenolpyruvate carboxylase: a comparative study between enzymes from monocot and eudicots, J. Mex. Chem. Soc. 56 (2012) 58–66.
[33] Y.H. Wang, M.G. Duff, L. Lepiniec, C. Crétin, G. Sarath, S.A. Condon, J. Vidal, P. Gadal, R. Chollet, Site-directed mutagenesis of the phosphorylatable serine (Ser8) in C4 phosphoenolpyruvate carboxylase from sorghum. The effect of negative charge at position 8, J. Biol. Chem. 267 (1992) 16759–16762.
[34] J.V. Olsen, S.E. Ong, M. Mann, Trypsin cleaves exclusively C-terminal to arginine and lysine residues, Mol. Cell. Proteomics 3 (2004) 608–614.
[35] N. Abramowitz, I. Schechter, A. Berger, On the size of the active site in proteases. II. Carboxypeptidase-A, Biochem. Biophys. Res. Commun. 29 (1967) 862–867.
[36] S.J. Hubbard, P. Argos, Cavities and packing at protein interfaces, Protein Sci. 3 (1994) 2194–2206.
[37] S.J. Hubbard, R.J. Beynon, J.M. Thornton, Assessment of conformational parameters as predictors of limited proteolytic sites in native protein structures, Protein Eng. Des. Sel. 11 (1998) 349–359.

[38] T. Šlechtová, M. Gilar, K. Kalíková, E. Tesařová, Insight into trypsin miscleavage: comparison of kinetic constants of problematic peptide sequences, Anal. Chem. 87 (2015) 7636–7764.
[39] B. Keil, Essential substrate residues for action of endopeptidases, in: Specificity of Proteolysis, Springer, Berlin, Heidelberg, 1992.
[40] J. Rodriguez, N. Gupta, R.D. Smith, P.A. Pevzner, Does trypsin cut before proline? J. Proteome Res. 7 (2008) 300–305.
[41] Y. Kai, H. Matsumara, T. Inoue, K. Terada, Y. Nagara, T. Yoshinaga, A. Kihara, K. Tsumura, K. Izui, Three-dimensional structure of phosphoenolpyruvate carboxylase: a proposed mechanism for allosteric inhibition, Proc. Natl. Acad. Sci. Unit. States Am. 96 (1999) 823–828.
[42] H. Matsumura, M. Terada, S. Shirakata, T. Inoue, T. Yoshinaga, K. Izui, Y. Kai, Plausible phosphoenolpyruvate binding site revealed by 2.6 Å structure of Mn^{2+}bound phosphoenolpyruvate carboxylase from *Escherichia coli*, FEBS Lett. 458 (1999) 93–96.
[43] H. Matsumura, Y. Xie, S. Shirakata, T. Inoue, T. Yoshinaga, Y. Ueno, Y.K. Izui, Y. Kai, Crystal structures of C4 from maize and quaternary complex of *E. coli* phosphoenolpyruvate carboxylases, Structure 10 (2002) 1721–1730.
[44] K. Izui, Kinetic studies on the allosteric nature of phosphoenolpyruvate carboxylase from *Escherichia coli*, J. Biochem. 68 (1970) 227–238.
[45] K. Izui, Effects of high pressure on the stability and activity of allosteric phosphoenolpyruvate carboxylase from *Escherichia coli*, Biochemistry 73 (1973) 505–513.
[46] H. Teraoka, K. Izui, H. Katsuki, Phosphoenolpyruvate carboxylase of *Escherichia coli*. Multiple conformational states elicited by allosteric effectors, Biochemistry 13 (1974) 5121–5128.
[47] C. Viappiani, S. Bettati, S. Bruno, L. Ronda, S. Abbruzzetti, A. Mozzarelli, W.A. Eaton, New insights into allosteric mechanisms from trapping unstable protein conformations in silica gels, Proc. Natl. Acad. Sci. Unit. States Am. 101 (2004) 14414–14419.
[48] W.A. Eaton, E.R. Henry, J. Hofrichter, S. Bettati, C. Viappiani, A. Mozzarelli, Evolution of allosteric models for hemoglobin, IUBMB Life 59 (2007) 586–599.
[49] N. Shibayam, K. Sugiyama, S.Y. Park, Structures and oxygen affinities of crystalline human hemoglobin C (β6 Glu->Lys) in the R and R2 quaternary structures, J. Biol. Chem. 286 (2011) 33661–33668.
[50] N. Shibayama, Allosteric transitions in hemoglobin revisited, Biochim. Biophys. Acta Gen. Subj. 1864 (2020) 129335.
[51] I. Bustos-Jaimes, M. Ramírez-Costa, L. De Anda-Aguilar, P. Hinojosa-Ocaña, M.L. Calcagno, Evidence for two different mechanisms triggering the change in quaternary structure of the allosteric enzyme, Glucosamine-6-phosphate deaminase, Biochemistry 44 (2005) 1127–1135.